

Bayesian sparsification for deep neural networks with Bayesian model reduction

Dimitrije Marković¹, Karl J. Friston^{3,4}, and Stefan J. Kiebel^{1,2}

¹Chair of Cognitive Computational Neuroscience, Technische Universität Dresden, 01062 Dresden, Germany.

²Centre for Tactile Internet with Human-in-the-Loop (CeTI), , Technische Universität Dresden, 01062 Dresden, Germany.

³Wellcome Centre for Human Neuroimaging, Queen Square Institute of Neurology, University College London, UK.

⁴VERSES AI Research Lab, Los Angeles, California, 90016, USA.

September 22, 2023

Abstract

Deep learning’s immense capabilities are often constrained by the complexity of its models, leading to an increasing demand for effective sparsification techniques. Bayesian sparsification for deep learning emerges as a crucial approach, facilitating the design of models that are both computationally efficient and competitive in terms of performance across various deep learning applications. The state-of-the-art – in Bayesian sparsification of deep neural networks – combines structural shrinkage priors on model weights with an approximate inference scheme based on black-box stochastic variational inference. However, model inversion of the full generative model is exceptionally computationally demanding, especially when compared to standard deep learning of point estimates. In this context, we advocate for the use of Bayesian model reduction (BMR) as a more efficient alternative for pruning of model weights. As a generalization of the Savage-Dickey ratio, BMR allows a post-hoc elimination of redundant model weights based on the posterior estimates under a straightforward (non-hierarchical) generative model. Our comparative study highlights the computational efficiency and the pruning rate of the BMR method relative to the established stochastic variational inference (SVI) scheme, when applied to the full hierarchical generative model. We illustrate the potential of BMR to prune model parameters across various deep learning architectures, from classical networks like LeNet to modern frameworks such as Vision Transformers and MLP-Mixers.

1 Introduction

Bayesian deep learning integrates the principles of Bayesian methodology with the objectives of deep learning, facilitating the training of expansive parametric models tailored for classifying and generating intricate audio-visual data, including images, text, and speech [Wang and Yeung, 2020, Wilson, 2020, Wang and Yeung, 2016]. Notably, the Bayesian approach frames the challenge of model optimization as an inference problem. This perspective is especially apt for scenarios necessitating decision-making under uncertainty [Murphy, 2022, Ghahramani, 2015]. As a result, Bayesian formulations in deep learning have proven advantageous in various respects, offering enhancements in generalization [Wilson and Izmailov, 2020], accuracy, calibration [Izmailov et al., 2020, Luo and Kareem, 2020], and model compression [Louizos et al., 2017].

These functional enhancements are intrinsically tied to judiciously chosen structural priors [Fortuin, 2022]. The priors, integral to the probabilistic generative model, scaffold the architecture of the network, thereby reducing the data required for the inference of optimal parametric solutions. Recent studies have highlighted the efficacy of hierarchical shrinkage priors over model weights, a specific category of structural priors, in achieving highly-sparse network representations [Nalisnick et al., 2019,

[Louizos et al., 2017, Seto et al., Ghosh et al., 2018]. Sparse representations not only reduce redundancy but also evince additional performance benefits. However, the adoption of shrinkage priors in all deep learning models presents a conundrum: the ballooning space of latent parameters and the diminishing scalability of prevailing approximate inference schemes [Snoek et al., 2015, Krishnan et al., 2019, Izmailov et al., 2020, Daxberger et al., 2021a].

In line with ongoing research on scalable Bayesian inference, we introduce an approximate inference scheme rooted in Bayesian model reduction (BMR). In essence, BMR extends the foundational principles of the Savage-Dickey Density Ratio method [Cameron, 2013]. BMR is typically conceptualized as a combinatorial model comparison framework, enabling swift estimations of model evidence across an extensive array of models, that differ in their prior assumptions, to identify the most probable one. Originally conceived for model comparison within the dynamical causal modeling framework [Rosa et al., 2012, Friston and Penny, 2011], the scope of BMR has since broadened. Subsequent works expanded its methodology [Friston et al., 2016, 2017, 2018] and adapted it for structure learning [Smith et al., 2020]. More recently, BMR has found applications in Bayesian nonlinear regression and classification tasks using Bayesian neural networks with variance backpropagation [Beckers et al., 2022, Haufmann et al., 2020].

The BMR method is intimately connected with the spike-and-slab prior, a type of shrinkage prior [Mitchell and Beauchamp, 1988]. Intriguingly, this specific structured shrinkage prior has parallels with Dropout regularization [Nalisnick et al., 2019]. Such an association spurred researchers in Bayesian deep learning to formulate sparsification methods based on a different type of shrinkage prior – the hierarchical horseshoe prior [Piironen and Vehtari, 2017] – as a tool for automated depth determination. Subsequent studies suggested that merging horseshoe priors with structured variational approximations yields robust, highly sparse representations [Ghosh et al., 2018]. The allure of continuous shrinkage priors (e.g., horseshoe priors) stems from the computational challenges associated with model inversion reliant on spike-and-slab priors [Nalisnick et al., 2019, Piironen and Vehtari, 2017]. However, continuous shrinkage priors necessitate a considerably more expansive parameter space, to represent the approximate posterior, compared to optimizing neural networks using the traditional point estimate method.

In this work, we reexamine the spike-and-slab prior within the framework of BMR-based sparsification, highlighting its efficiency. Notably, this approach circumvents the need to expand the approximate posterior beyond the conventional fully factorised mean-field approximation, making it more scalable than structured variational approximations [Ghosh et al., 2018]. In this light, BMR can be seen as a layered stochastic and black-box variational inference technique, which we term *stochastic BMR*. We subject the stochastic BMR to rigorous validation across various image classification tasks and network architectures, including LeNet-5 [LeCun et al., 1989], Vision Transformers [Dosovitskiy et al., 2020], and MLP-Mixers [Tolstikhin et al., 2021].

Central to our study is an empirical comparison of stochastic BMR with methods anchored in hierarchical horseshoe priors. Through multiple metrics - from Top-1 accuracy to expected calibration error and negative log-likelihood - we establish the competitive performance of stochastic BMR. We argue its computational efficiency, and remarkable sparsification rate, position BMR as an appealing choice, enhancing the scalability and proficiency of contemporary deep learning networks across diverse machine learning challenges, extending well beyond computer vision. We conclude with a discussion on potential avenues of future research that could further facilitate of BMR based pruning of deep neural networks.

2 Methods

2.1 Variational inference

Given a joint density of latent variables, represented as $\mathbf{z} = (z_1, \dots, z_k)$, and a dataset of n observations $\mathcal{D} = (y_1, \dots, y_n)$ we can express the joint density, that is, the generative model, as

$$p(\mathcal{D}, \mathbf{z}) = p(\mathbf{z}) p(\mathcal{D}|\mathbf{z}). \quad (1)$$

The posterior density is then obtained, following the Bayes rule, as

$$p(\mathbf{z}|\mathcal{D}) \propto p(\mathbf{z}) p(\mathcal{D}|\mathbf{z}). \quad (2)$$

For complex generative models, direct inference as described above becomes computationally prohibitive. To circumvent this, we approximate the exact posterior $p(\mathbf{z}|\mathcal{D})$, constraining it to a distribution $q(z)$ that belongs to a named distribution family \mathcal{Q} . We then seek $q^*(z) \in \mathcal{Q}$, an approximate solution that minimizes the following Kullback-Leibler divergence [Blei et al., 2017]

$$q^*(z) = \underset{q \in \mathcal{Q}}{\operatorname{argmin}} D_{KL} \left(q(z) \parallel p(\mathbf{z}|\mathcal{D}) \right) = \underset{q \in \mathcal{Q}}{\operatorname{argmin}} F[q], \quad (3)$$

where $F[q]$ stands for the variational free energy (VFE), defined as

$$F[q] = E_{q(\mathbf{z})} [\ln q(\mathbf{z}) - \ln p(\mathcal{D}, \mathbf{z})] \quad (4)$$

VFE serves as an upper bound on the marginal log-likelihood

$$F[q] = D_{KL} \left(q(\mathbf{z}) \parallel p(\mathbf{z}|\mathcal{D}) \right) - \ln p(\mathcal{D}) \geq -\ln p(\mathcal{D})$$

As KL-divergence is always greater or equal to zero, minimizing VFE brings the approximate solution as close as possible to the true posterior, without having to compute the exact posterior.

The most straightforward way to obtain the approximate posterior $q^*(z)$, is to minimize the VFE along its negative gradient:

$$\dot{\phi} = -\nabla_{\phi} F[q]$$

where ϕ signifies the parameters of the approximate posterior $q_{\phi}(\mathbf{z}) = q(\mathbf{z}|\phi)$. Thus, variational inference reframes the inference problem highlighted in eq. (2) as an optimization problem Beal [2003].

2.2 Stochastic and black-box variational inference

Stochastic variational inference (SVI) improves the computational efficiency of gradient descent by approximating the variational free energy using a subset $\mathcal{K}_i = (y_{s_1^i}, \dots, y_{s_k^i})$; $k \ll n$ – of the entire data set \mathcal{D} . This approach fosters a stochastic gradient descent (SGD) mechanism, capable of managing large datasets [Hoffman et al., 2013]. Crucially, at every iteration step i of the SGD process, the subset \mathcal{K}_i undergoes re-sampling.

Black-box Variational Inference (BBVI) facilitates the optimization of any (named or unnamed) posterior density $q_{\phi}(\mathbf{z})$, through the integration of Monte Carlo estimates for variational gradients [Ranganath et al., 2014]. This can be formulated as

$$\nabla_{\phi} F[q] \approx \nabla_{\phi} \hat{F}[q] = \frac{1}{S} \sum_{s=1}^S \nabla_{\phi} \ln q_{\phi}(\mathbf{z}) \left[\ln \frac{q_{\phi}(\mathbf{z})}{q_{\phi}(\mathbf{z})} + 1 \right] \quad \mathbf{z}_s \sim q(\mathbf{z}|\phi) \quad (5)$$

To mitigate the variance inherent to Monte Carlo gradient estimations, we employ Rao-Blackwellization [Schulman et al., 2015], with an implementation sourced from NumPyro [Bingham et al., 2019]. For optimizing the variational objective stochastically, we leverage the AdaBelief optimizer [Zhuang et al., 2020]. As an adaptive algorithm, AdaBelief ensures swift convergence, robust generalization, and steady optimization. Notably, we utilize AdaBelief’s implementation from the Optax package within the JAX ecosystem [Babuschkin et al., 2020].

2.3 Bayesian model reduction

Let us consider two generative processes for the data: a full (i.e., flat) model

$$p(\mathbf{z}|\mathcal{D}) \propto p(\mathcal{D}|\mathbf{z}) p(\mathbf{z}) \quad (6)$$

and a reduced model in which the flat prior $p(\mathbf{z})$ is replaced with a more informative prior $\tilde{p}(\mathbf{z}) = p(\mathbf{z}|\mathbf{z}_H)$ that depends on hyper-parameters \mathbf{z}_H . This change leads to a different posterior

$$\tilde{p}(\mathbf{z}|\mathcal{D}) \propto p(\mathcal{D}|\mathbf{z}) \tilde{p}(\mathbf{z}) \quad (7)$$

Noting that as the following relation holds:

$$1 = \int d\mathbf{z} \tilde{p}(\mathbf{z}|\mathcal{D}) = \int d\mathbf{z} p(\mathbf{z}|\mathcal{D}) \frac{\tilde{p}(\mathbf{z}) p(\mathcal{D})}{p(\mathbf{z}) \tilde{p}(\mathcal{D})},$$

we can express the link between the models as:

$$\begin{aligned} -\ln \tilde{p}(\mathcal{D}) &= -\ln p(\mathcal{D}) - \ln \int dz p(\mathbf{z}|\mathcal{D}) \frac{\tilde{p}(\mathbf{z})}{p(\mathbf{z})} \\ &\approx F(\phi^*) - \ln \int dz q_{\phi^*}(\mathbf{z}) \frac{\tilde{p}(\mathbf{z})}{p(\mathbf{z})} \end{aligned} \quad (8)$$

where we assumed the approximate posterior for the full model corresponds to $p(\mathbf{z}|\mathcal{D}) \approx q_{\phi^*}(\mathbf{z})$, and that $-\ln p(\mathcal{D}) \approx F(\phi^*)$.

From eq. (8) we obtain the free energy of the reduced model as

$$-\ln \tilde{p}(\mathcal{D}) \approx -\ln E_q \left[\frac{\tilde{p}(\mathbf{z})}{p(\mathbf{z})} \right] + F(\phi^*) = -\Delta F(\mathbf{z}_H). \quad (9)$$

where $\Delta F(\mathbf{z}_H)$ denotes the change in the free energy of going from the full model to the reduced model, given hyper-parameters \mathbf{z}_H . Note that for $\Delta F(\mathbf{z}_H) > 0$ the reduced model has a better variational free energy compared to the flat model. Consequently, the reduced model offers a model with a greater marginal likelihood; i.e., a better explanation for the data and improved generalization capabilities. Heuristically, this can be understood as minimising model complexity, without sacrificing accuracy (because log evidence can be expressed as accuracy minus complexity, where complexity is the KL divergence between posterior and prior beliefs). This relationship is pivotal in formulating efficient pruning criteria, especially for extensive parametric models commonly employed in deep learning.

2.4 Bayesian neural networks

In a general (nonlinear) regression problem, we model the relationship between predictors $\mathbf{X} = (\mathbf{x}_1, \dots, \mathbf{x}_n)$ and target variables $\mathbf{Y} = (\mathbf{y}_1, \dots, \mathbf{y}_n)$ using a likelihood distribution from an exponential family as

$$\mathbf{y}_i \sim p(\mathbf{y}|\mathcal{W}, \mathbf{x}_i) = h(y) \exp \left[\boldsymbol{\eta}(\mathbf{f}(\mathcal{W}, \mathbf{x}_i)) \cdot \mathbf{T}(\mathbf{y}) - A(\mathbf{f}(\mathcal{W}, \mathbf{x}_i)) \right]. \quad (10)$$

Functions $h(\cdot)$, $\boldsymbol{\eta}(\cdot)$, $\mathbf{T}(\cdot)$, $A(\cdot)$ are known and selected depending on the task. For example in a regression problem the likelihood will correspond to a multivariate normal distribution and in a classification problem to a categorical distribution. In this work, we will only consider a categorical likelihood, as it is the most suitable for image classification tasks.

The mapping $\mathbf{f}(\mathcal{W}, \mathbf{x}_i)$ represents a generic deep neural network of depth L defined as

$$\begin{aligned} \mathcal{W} &= (\mathbf{W}_1, \dots, \mathbf{W}_L) \\ \mathbf{h}_i^0 &= \mathbf{x}_i \\ \mathbf{h}_i^l &= \mathbf{g} \left(\mathbf{W}_l \cdot \left[\mathbf{h}_i^{l-1}; 1 \right] \right) \\ \mathbf{f}(\mathcal{W}, \mathbf{x}_i) &= \mathbf{W}_L \cdot \left[\mathbf{h}_i^{L-1}; 1 \right] \end{aligned} \quad (11)$$

A probabilistic formulation of the deep learning task, that is, inferring model weights, introduces implicit bias to the parameters \mathcal{W} of an artificial neural network in the form of a prior distribution $p(\mathcal{W})$. Hence, parameter estimation is cast as an inference problem where

$$p(\mathcal{W}|\mathcal{D}) \propto p(\mathcal{W}) \prod_{i=1}^n p(\mathbf{y}_i|\mathcal{W}, \mathbf{x}_i) \quad (12)$$

The choice of the prior distribution is crucial for optimal task performance, and a prior assumption of structural sparsity is essential for inferring sparse representations of over-parameterised models, such as deep neural networks.

2.5 Bayesian neural networks with shrinkage priors

Shrinkage priors instantiate a prior belief about the sparse structure of model parameters. Here, we will investigate two well-established forms of shrinkage priors for network weight parameters, a canonical

spike-and-slab prior [George and McCulloch, 1993, Mitchell and Beauchamp, 1988] defined as

$$\begin{aligned} w_{ijl} &\sim \mathcal{N}\left(0, \lambda_{ijl}^2 \gamma_0^2\right) \\ \lambda_{ijl} &\sim \text{Bernoulli}(\pi_l) \\ \pi_l &\sim \mathcal{B}e(\alpha_0, \beta_0) \end{aligned} \tag{13}$$

and a regularised-horseshoe prior [Piironen and Vehtari, 2017]

$$\begin{aligned} w_{ijl} &\sim \mathcal{N}\left(0, \gamma_{il}^2\right) \\ \gamma_{il}^2 &= \frac{c_l^2 v_l^2 \tau_{il}^2}{c_l^2 + \tau_{il}^2 v_l^2} \\ c_l^{-2} &\sim \Gamma(2, 6) \\ \tau_{il} &\sim \mathcal{C}^+(0, 1) \\ v_l &\sim \mathcal{C}^+(0, \tau_0) \end{aligned} \tag{14}$$

where $i \in \{1, \dots, K_l\}$, $j \in [1, \dots, K_{l-1} + 1]$, and where w_{ijl} denotes ij th element of the weight matrix at depth l . The symbols $\mathcal{B}e$, and \mathcal{C}^+ denote a Beta distribution and a half-Cauchy distribution, respectively.

Importantly, the spike-and-slab prior relates to dropout regularisation, which is commonly introduced as a sparsification method in deep learning [Nalisnick et al., 2019, Mobiny et al., 2021]. This type of prior is considered the gold standard in shrinkage priors and has been used in many recent applications of Bayesian sparsification on neuronal networks [Bai et al., 2020, Hubin and Storvik, 2023, Jantre et al., 2021, Sun et al., 2022, Ke and Fan, 2022] showing excellent sparsification rates. However, the inversion of the resulting hierarchical model is challenging and requires carefully constructed posterior approximations. Moreover, their dependence on discrete random variables renders them unsuitable for Markov-Chain Monte Carlo-based sampling schemes. As a result, researchers often use continuous formulations of the shrinkage-prior, with the horseshoe prior being a notable example.

In contexts that involve sparse learning with scant data, the regularised horseshoe prior has emerged as one of the preferred choices within shrinkage prior families [Ghosh et al., 2019]. A distinct advantage of this prior is its ability to define both the magnitude of regularisation for prominent coefficients and convey information about sparsity. It is worth noting a dependency highlighted in Ghosh et al. [2018]: for $v_l \tau_{il} \ll 1$ the equation simplifies to $\gamma_{il} \approx v_l \tau_{il}$ recovering the original horseshoe prior. In contrast, for $v_l \tau_{il} \gg 1$, the equation becomes $\gamma_{il}^2 \approx c_l^2$. In this latter scenario, the prior over the weights is defined as $w_{ijl} \sim \mathcal{N}(0, c_l^2)$, with c_l serving as a weight decay hyper-parameter for layer l .

2.6 Approximate posterior for Bayesian neural networks

To benchmark stochastic BMR, we explore two forms of prior distribution $p(\mathcal{W})$ — a flat and a hierarchical structure — in conjunction with a fully factorised mean-field approximation.

Firstly, let us consider the flat prior over model weights, represented in a non-centered parameterization:

$$\begin{aligned} \hat{w}_{ijl} &\sim \mathcal{N}(0, 1) \\ w_{ijl} &= \gamma_0 \hat{w}_{ijl} \end{aligned} \tag{15}$$

where we set $\gamma_0 = 0.1$. Based on this, we describe a fully factorised approximate posterior as:

$$\begin{aligned} q(\mathcal{W}) &= \prod_l \prod_i \prod_j q(\hat{w}_{ijl}) \\ q(\hat{w}_{ijl}) &= \mathcal{N}\left(\mu_{ijl}, \sigma_{ijl}^2\right). \end{aligned} \tag{16}$$

When inverting a hierarchical generative model over weights of artificial neural network, we exclusively apply stochastic black-box variational inference to the model variant with the regularised horseshoe prior. This choice is motivated by its documented superiority over the spike-and-slab prior,

as established in Ghosh et al. [2018]. We express the hierarchical prior in the non-centered parameterization as:

$$\begin{aligned}
a_{il}, b_{il} &\sim \Gamma\left(\frac{1}{2}, 1\right) \\
\hat{a}_l, \hat{b}_l &\sim \Gamma\left(\frac{1}{2}, 1\right) \\
\tau_{il} &= \sqrt{\frac{a_{il}}{b_{il}}} \\
v_l &= \tau_0 \sqrt{\frac{\hat{a}_l}{\hat{b}_l}} \\
\hat{w}_{ijl} &\sim \mathcal{N}(0, 1) \\
w_{ijl} &= \gamma_{il} \hat{w}_{ijl}
\end{aligned} \tag{17}$$

Note that the expressions above involve a reparameterization of Half-Cauchy distributed random variables as the square-root of the quotient of two Gamma distributed random variables, a strategy drawn from Wand et al. [2011] (see Reparameterisation for additional details). Such a reparameterization of the Half-Cauchy ensures capturing of fat-tails in the posterior, even when leveraging a fully-factorised mean-field posterior approximation, as referenced in Ghosh et al. [2018].

For the fully-factorised mean-field approximation, the approximate posterior is portrayed as a composite of Normal and Log-Normal distributed random variables, expressed as:

$$\begin{aligned}
q(c_l) &= \mathcal{LN}\left(\mu_{c,l}, \sigma_{c,l}^2\right) \\
q(\hat{a}_l) &= \mathcal{LN}\left(\hat{\mu}_{a,l}, \hat{\sigma}_{a,l}^2\right) \\
q(\hat{b}_l) &= \mathcal{LN}\left(\hat{\mu}_{b,l}, \hat{\sigma}_{b,l}^2\right) \\
q(a_{il}) &= \mathcal{LN}\left(\mu_{a,il}, \sigma_{a,il}^2\right) \\
q(b_{il}) &= \mathcal{LN}\left(\mu_{b,il}, \sigma_{b,il}^2\right) \\
q(\hat{w}_{ijl}) &= \mathcal{N}\left(\mu_{w,ijl}, \sigma_{w,ijl}^2\right)
\end{aligned} \tag{18}$$

2.7 Application of stochastic BMR to Bayesian neural networks

To apply BMR to Bayesian neural networks, we commence by estimating an approximate posterior for the flat model, as detailed in eq. (15). To retain high computational efficiency, we pair BMR solely with the fully factorised approximate posterior, as presented in eq. (16). While it is feasible to use this method alongside the structured posterior [Ghosh et al., 2018], it requires considerably more computationally intensive estimations of the reduced free energy. As shown below, we obtain satisfactory results with a fully factorised posterior. Therefore, we defer the exploration of BMR with a structured posterior to future endeavours.

Given a fully factorised approximate posterior, we can determine the change in variational free energy, ΔF — after substituting the prior $\mathcal{N}(0, 1)$ with $\mathcal{N}(0, \theta_{ijl}^2)$ for the weight \hat{w}_{ijl} — as:

$$\begin{aligned}
\Delta F(\theta_{ijl}) &= -\frac{1}{2} \ln \rho_{ijl}^2 - \frac{1}{2} \frac{\mu_{ijl}^2}{\sigma_{ijl}^2} \left(1 - \frac{\theta_{ijl}^2}{\rho_{ijl}^2}\right) \\
\rho_{ijl}^2 &= \theta_{ijl}^2 + \sigma_{ijl}^2 - \theta_{ijl}^2 \sigma_{ijl}^2
\end{aligned} \tag{19}$$

For the second hierarchical level of the approximate posterior, we aim to minimize the following form for the variational free energy:

$$F = \sum_{l=1}^L E_{q(\boldsymbol{\theta}_l)} \left[-\sum_{i,j} \Delta F(\theta_{ijl}) + \ln \frac{q(\boldsymbol{\theta}_l)}{p(\boldsymbol{\theta}_l)} \right] \tag{20}$$

This minimization is done with respect to $q(\Theta) = \prod_l q(\theta_l)$, the approximate posterior over hyper-parameters. Note the application of eq. (9) in substituting the marginal log-likelihood with the change in the variational free energy.

For the spike-and-slab prior we can write the following relation:

$$\begin{aligned} \theta_l &= [\pi_l, \lambda_{ijl}] \text{ for } i \in \{1, \dots, K_l\}, \text{ and } j \in \{1, \dots, K_{l-1} + 1\} \\ \theta_{ijl} &= \lambda_{ijl} \end{aligned}$$

Consequently, the approximate posterior at the second level of the hierarchy can be approximated as:

$$\begin{aligned} q(\Theta) &= \prod_l q(\pi_l) \prod_{ij} q(\lambda_{ijl}) \\ q(\lambda_{ijl}) &= q_{ijl}^{\lambda_{ijl}} (1 - q_{ijl})^{1 - \lambda_{ijl}} \\ q(\pi_l) &= \mathcal{B}(\alpha_l, \beta_l) \end{aligned} \tag{21}$$

The iterative update to obtain the minimum of the simplified variational free energy (eq. (20)) is then:

$$\begin{aligned} q_{ijl}^{k+1} &= \frac{1}{1 + e^{-[\zeta_l^k - \Delta F(\lambda_{ijl}=0)]}} \\ \zeta_l^k &= \psi(\alpha_l^k) - \psi(\beta_l^k) \\ \alpha_l^{k+1} &= \sum_{i,j} q_{ijl}^{k+1} + \alpha_0 \\ \beta_l^{k+1} &= \sum_{i,j} (1 - q_{ijl}^{k+1}) + \beta_0 \end{aligned} \tag{22}$$

Here, $\alpha_l^0 = \alpha_0$, $\beta_l^0 = \beta_0$, $\Delta F(\lambda_{ijl}=0) = -\frac{1}{2} \left[\ln \sigma_{ijl}^2 + \frac{\mu_{ijl}^2}{\sigma_{ijl}^2} \right]$, and $\psi(\cdot)$ refers to the digamma function. The efficiency of this inference scheme is remarkable, typically achieving convergence after a few iterations. In practice, we cap the maximum number of iterations at $k_{max} = 4$.

Finally, we use the following pruning heuristics to eliminate model weights and sparsify network structure

$$\text{if } q_{ijl}^{k_{max}} < \frac{1}{2}, \text{ set } \hat{w}_{ijl} = 0. \tag{23}$$

To achieve the high sparsification rate presented in the next section, we adopt an iterative optimisation and pruning approach proposed in Beckers et al. [2022]. After initial convergence of the SVI, for the flat prior, and fully factorised posterior (capped at 10^5 iterations) we perform weight pruning, and further optimisation for $2 \cdot 10^4$ iterations, completing one epoch. In total, we apply iterative pruning and optimisation for five epochs in all examples below.

The complete implementation of stochastic BMR is available at an online repository github.com/dimarkov/bmr4pml with notebooks and scripts necessary to recreate all result figures.

3 Results

3.1 Performance Comparison

We assessed the performance of four deep neural network (DNN) architectures: MLP, LeNet-5, Mlp-Mixer, and a variant of the Vision Transformer (detailed in [Specification of neural network architectures](#)). Our evaluations covered standard image classification benchmarks, including Fashion MNIST, CIFAR10, and CIFAR100. We quantified performance using top-1 accuracy (ACC), expected calibration error (ECE), and negative log likelihood (NLL) determined from the test data. While top-1 accuracy is a straightforward measure of model performance, it provides only limited information. ECE and NLL complement the accuracy measure by characterising the model’s confidence, and predictability of new labels, respectively. In practice, a good overall performance corresponds to high ACC, and low ECE and NLL.

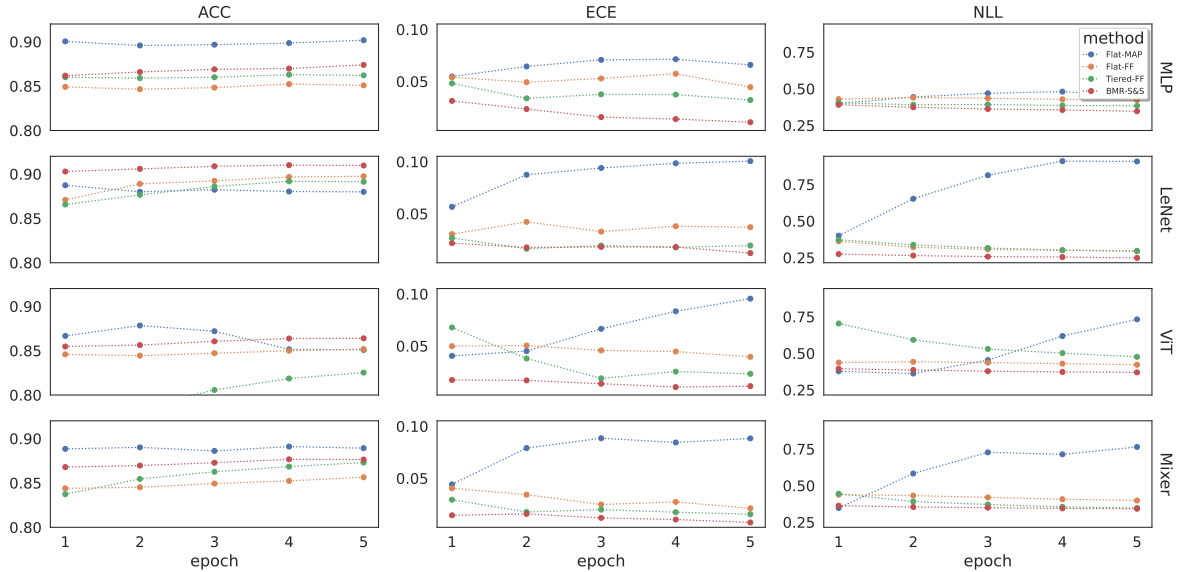


Figure 1: Classification performance comparison on FashionMNIST dataset for different neuronal architectures and approximate inference schemes.

The training regimen used a batch size of $N_B = 128$ and the default settings of the AdaBelief algorithm ($\alpha = 10^{-3}$, $\beta_1 = 0.9$, $\beta_2 = 0.999$) as detailed in Zhuang et al. [2020]. Figure 1 charts the epoch-wise evolution of ACC, ECE, and NLL for each architecture, under five distinct approximate inference strategies: (i) Maximum a posteriori (MAP) estimate for the flat generative model, akin to traditional deep learning point estimates coupled with weight decay. (ii) A fully factorised posterior approximation for the flat generative model (Flat-FF). (iii) A fully factorised posterior approximation of the hierarchical generative model with a regularised horseshoe prior (Tiered-FF). (iv) The stochastic BMR algorithm augmented with a spike-and-slab prior (BMR-S&S). Each epoch is defined by $20K$ stochastic gradient steps, with each step randomly drawing N_B data instances from the training pool.

Interestingly, all approximate inference methods demonstrate comparable top-1 accuracy scores. However, the stochastic BMR method followed by the Tiered-FF approximation, consistently resulted in the lowest ECE and NLL scores across all DNN architectures and datasets (see Figure S1 for CIFAR10 dataset and Figure S2 for CIFAR100 dataset). The implicit reduction in model complexity suggests that—as anticipated—Stochastic BMR furnishes a model of the data that has the greatest evidence or marginal likelihood (not shown). In this setting, the NLL of the test data can be regarded as a proxy for (negative log) marginal likelihood.

3.2 Learning of sparse representations

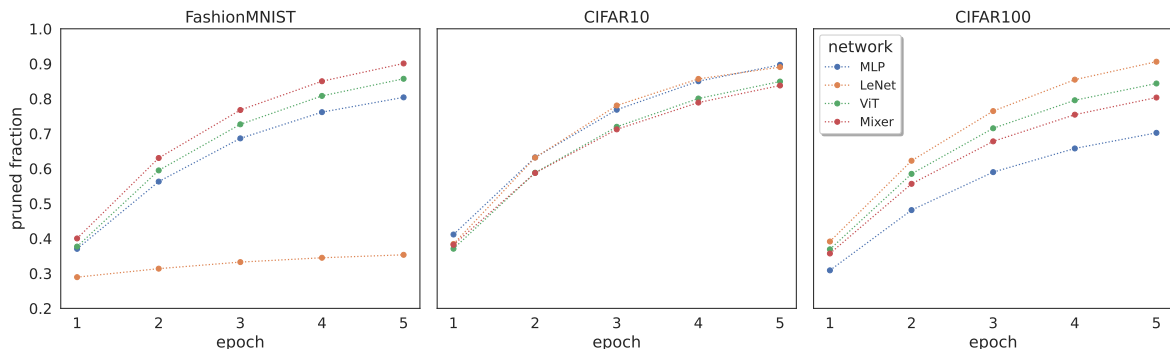


Figure 2: Total fraction of pruned model parameters obtained with the stochastic BMR algorithm across different DNN architectures and datasets.

Figure 2 depicts the fraction of pruned model parameters for different DNN architectures and datasets. It is noteworthy to observe the substantive sparsity achieved by the stochastic BMR algorithm. This sparsity is consistent across datasets and architectures, with the exception of the LeNet-5 structure when used for the FashionMNIST dataset, because by default LeNet-5 architecture is already sparse and contains relatively low-number of model weights (for other data sets we substantially increased the dimensionality of hidden layers as detailed in [Specification of neural network architectures](#)).

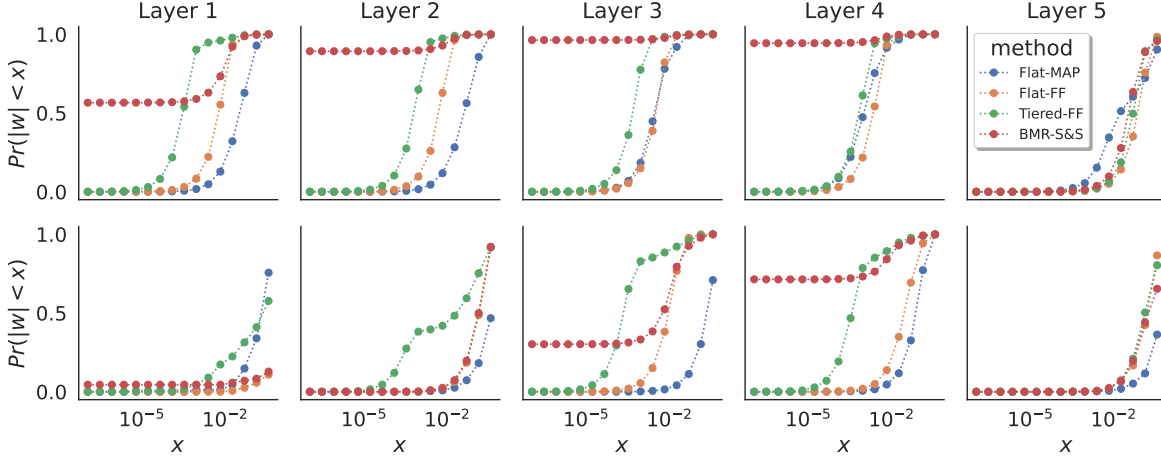


Figure 3: Cumulative Distribution Function (CDF) of absolute posterior parameter expectations at different layers of MLP (top row), and LeNet architectures (bottom row). The y-axis represents the fraction of parameters with values less than or equal to the value on the x-axis.

To delve deeper into the pruning behavior across varying network depths, Figure 3 presents a per-layer cumulative distribution function (CDF) for model parameters, highlighting the proportion of parameters whose absolute mean posterior estimate falls below a given threshold. When juxtaposing the BMR CDF trajectories with those obtained from the Tiered-FF method (sparsification is induced by the regularised half-cauchy prior), it is evident that BMR furnishes more pronounced sparsification. This distinction is crucial, as the stochastic BMR not only matches or surpasses the performance of the Tiered-FF algorithm but also averages a 15% faster stochastic gradient descent.

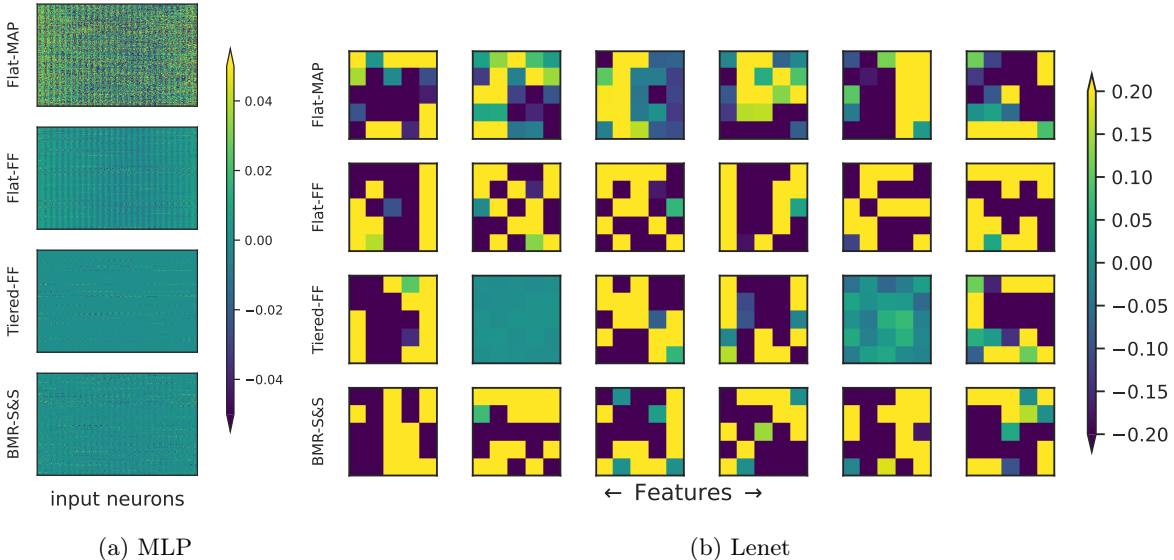


Figure 4: Posterior expectations (color coded) over model parameters obtained using different approximate inference schemes at the first layer of (a) MLP architecture, and (b) LeNet architectures.

To illustrate the structural learning variations among algorithms, Figure 4 presents heatmaps of

posterior expectations obtained using the four different methods. The Figure 4 reveals subtle differences between inferred representations of the MLP and LeNet-5 architecture’s input layers trained on the Fashion MNIST dataset. Divergent compression rates among the algorithms indicate inherent trade-offs between efficiency and performance. It is evident that the stochastic BMR strikes a balance between compression advantages and performance, as it is less prone to over-pruning as compared to the Tiered-FF method (two featured of the LeNet-5 input layer are effectively removed - see Figure 4(b)).

4 Discussion

In this study, we presented a novel algorithm – stochastic Bayesian model reduction – designed for an efficient Bayesian sparsification of deep neural networks. Our proposed method seamlessly integrates stochastic and black-box variational inference with Bayesian model reduction (BMR), a generalisation of the Savage-Dickey ratio. Through the stochastic BMR strategy, we enable iterative pruning of model parameters, relying on posterior estimates acquired from a straightforward variational mean-field approximation to the generative model. This model is characterized by Gaussian priors over individual parameters and layer-specific scale parameters. The result is an efficient pruning algorithm for which the computational demand of the pruning step is negligible compared to the direct stochastic black-box optimization of the full hierarchical model.

Over recent years, the Bayesian sparsification of neural networks has gained momentum, primarily driven by the spike-and-slab prior [Bai et al. \[2020\]](#), [Hubin and Storvik \[2023\]](#), [Jantre et al. \[2021\]](#), [Sun et al. \[2022\]](#), [Ke and Fan \[2022\]](#). These works have showcased the remarkable sparsification capabilities inherent to such shrinkage priors. Nevertheless, when juxtaposed with the stochastic BMR algorithm, they often necessitate supplementary assumptions related to the approximate posterior. These assumptions, in turn, lead to a more computation-intensive model inversion. Moreover, in contrast to related approaches, the versatility of stochastic BMR allows its integration with more efficient optimization techniques, like variational Laplace [Daxberger et al. \[2021b\]](#) and proximal-gradient methods [Khan et al. \[2018\]](#), provided the resulting approximate posterior in the form of a normal distribution is apt for the application at hand.

The insights obtained here pave the way for a deeper exploration of the potential applications of Bayesian model reduction across a wider array of architectures and tasks in probabilistic machine learning, such as audiovisual and natural language processing tasks. A more detailed fine tuning of the core dynamics of these algorithms, in terms of iterations steps, learning rates, and other free-parameters, might be the key to unveiling even more proficient Bayesian deep learning methodologies in the near future.

4.1 Acknowledgments

We would like to thank Conor Heins, Magnus Koudahl, and Beren Millidge for valuable discussions during the initial stages of this work.

4.2 Funding statement

SK acknowledges support by DFG TRR 265/1 (Project ID 402170461, B09) and Germany’s Excellence Strategy – EXC 2050/1 (Project ID 390696704) – Cluster of Excellence “Centre for Tactile Internet with Human-in-the-Loop” (CeTI) of Technische Universität Dresden.

A Specification of neural network architectures

For the simple multi-layer perceptron, we configure the architecture with five hidden layers, each comprising 400 neurons. The chosen activation function is the Swish activation function [[Ramachandran et al., 2017](#)].

For the LeNet-5 architecture, we adhere to the original design, which includes three convolutional layers, average pooling following the initial two convolutional layers, and two linear layers. The activation function used is the hyperbolic tangent. The convolutional layers employ a kernel size of 5×5 , while the average pooling uses a window of shape 2×2 . For the FashionMNIST dataset, the feature counts of the convolutional layers are designated as (6, 16, 120), and the two linear layers have neuron

counts of (84, 10). However, for the CIFAR10 and CIFAR100 datasets, we elevate the feature counts of the convolutional layers to (18, 48, 360), with linear layer neuron counts set to (256, 10) for CIFAR10 and (256, 100) for CIFAR100.

For the MlpMixer architecture we employ six layers and a patch resolution of 4×4 . Across all datasets, we maintain constant values for hidden size (C), sequence length (S), MLP channel dimension (D_C), and MLP token dimension (D_S); specifically $C = 256$, $S = 64$, $D_C = 512$ and $D_S = 512$ for all datasets.

For the VisionTransformer architecture, we adopt a slightly modified version of the ViT-Tiny setup: we use six layers, eight heads for each attention block, an embedding dimension of 256, and a hidden dimension of 512. The patch resolution of 4×4 is consistent with the MlpMixer. In both MlpMixer and VisionTransformer architectures, the GeLU activation function is utilized [Hendrycks and Gimpel, 2016].

For training using the maximum a posteriori estimate (Flat-MAP), dropout regularization, with dropout probability set to 0.2, is applied to all linear layers across all architectures, with the exception of the MlpMixer.

B Reparameterisation

In the centered parameterization of a generative model, Stochastic Variational Inference (SVI) with a fully factorized posterior yields a non-sparse solution, undermining the objective of employing shrinkage priors [Ghosh et al., 2019]. Typically, this limitation is addressed by adopting the non-centered parameterization of the prior.

Consider the unique property of the half-Cauchy distribution: given $x \sim \mathcal{C}^+(0, 1)$, and $z = bx$ the resulting probability distribution for z is $z \sim \mathcal{C}^+(0, b)$. Therefore, the non-centred parameterization is formulated as

$$\begin{aligned} \hat{\tau}_i^l &\sim \mathcal{C}^+(0, 1) \\ \hat{\lambda}_{ij}^l &\sim \mathcal{C}^+(0, 1) \\ \hat{w}_{ij}^l &\sim \mathcal{N}(0, 1) \\ \left[\gamma_{ij}^l\right]^2 &= \frac{\left[c^l \tau_0^l \hat{\tau}_i^l \hat{\lambda}_{ij}^l\right]^2}{\left[c^l\right]^2 + \left[\tau_0^l \hat{\tau}_i^l \hat{\lambda}_{ij}^l\right]^2} \\ w_{ij}^l &= \gamma_{ij}^l \hat{w}_{ij}^l \end{aligned} \tag{24}$$

However, while the half-Cauchy distribution is frequently chosen for sampling-based inference, it poses challenges in variational inference [Piironen and Vehtari, 2017]. Firstly, exponential family-based approximate posteriors (e.g., Gamma or log-Normal distributions) inadequately capture the half-Cauchy distribution’s fat tails. Secondly, using a Cauchy approximating family for the posterior results in high variance gradients during stochastic variational inference [Ghosh et al., 2019]. Hence, in the context of stochastic variational inference, the half-Cauchy distribution undergoes a reparameterization, as described in [Ghosh et al., 2018]:

$$x \sim \mathcal{C}^+(0, b) \equiv x = \sqrt{\frac{1}{u}}, u \sim \Gamma\left(\frac{1}{2}, \frac{1}{v}\right), v \sim \Gamma\left(\frac{1}{2}, b^2\right) \tag{25}$$

or, when represented in the non-centered parameterization:

$$x = b\sqrt{\frac{v}{u}}, u \sim \Gamma\left(\frac{1}{2}, 1\right), v \sim \Gamma\left(\frac{1}{2}, 1\right) \tag{26}$$

C Supplementary Material

References

Hao Wang and Dit-Yan Yeung. A survey on bayesian deep learning. *ACM Computing Surveys (CSUR)*, 53(5):1–37, 2020.

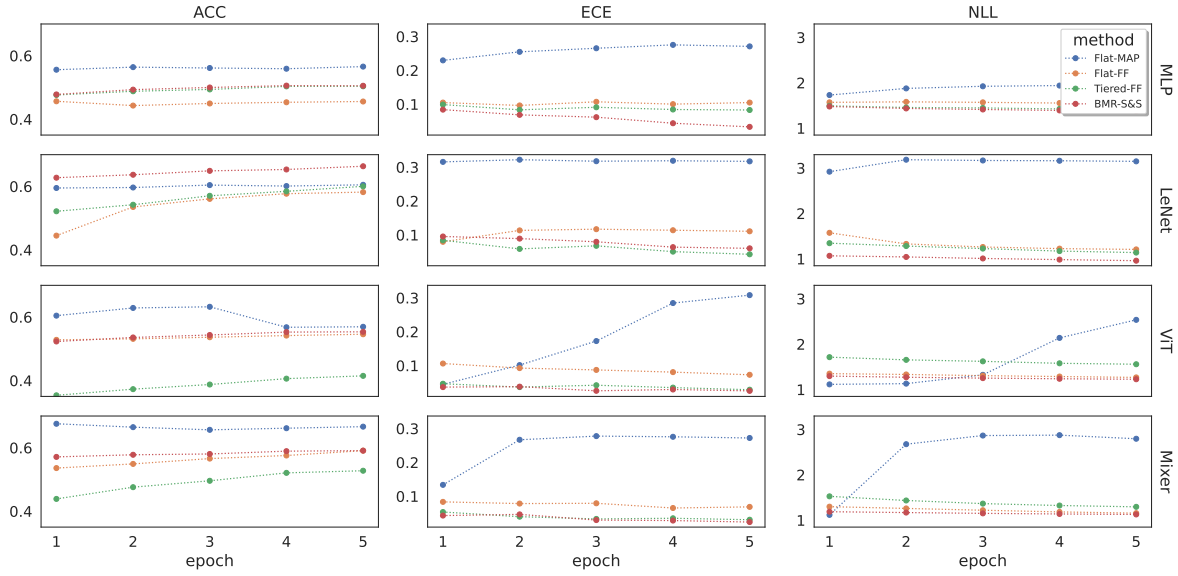


Figure S1: Classification performance comparison on CIFAR10 dataset for different neuronal architectures and approximate inference schemes.

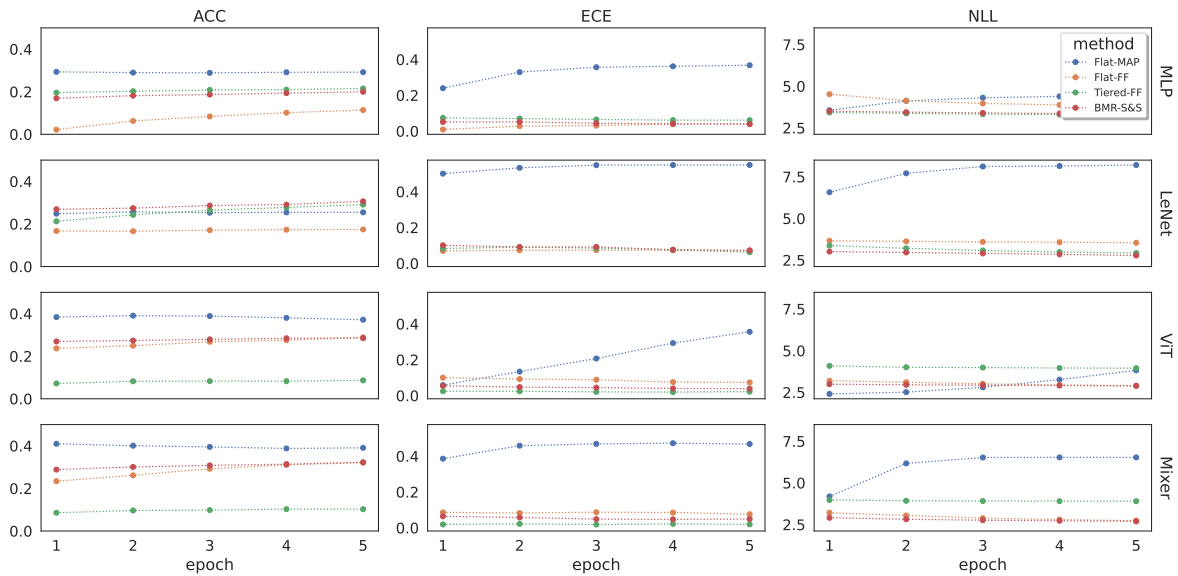


Figure S2: Classification performance comparison on CIFAR100 dataset for different neuronal architectures and approximate inference schemes.

Andrew Gordon Wilson. The case for bayesian deep learning, 2020. URL <https://arxiv.org/abs/2001.10995>.

Hao Wang and Dit-Yan Yeung. Towards bayesian deep learning: A framework and some existing methods. *IEEE Transactions on Knowledge and Data Engineering*, 28(12):3395–3408, 2016.

Kevin P Murphy. *Probabilistic machine learning: an introduction*. MIT press, 2022.

Zoubin Ghahramani. Probabilistic machine learning and artificial intelligence. *Nature*, 521(7553): 452–459, 2015.

Andrew G Wilson and Pavel Izmailov. Bayesian deep learning and a probabilistic perspective of generalization. In H. Larochelle, M. Ranzato, R. Hadsell, M.F. Balcan, and H. Lin,

- editors, *Advances in Neural Information Processing Systems*, volume 33, pages 4697–4708. Curran Associates, Inc., 2020. URL <https://proceedings.neurips.cc/paper/2020/file/322f62469c5e3c7dc3e58f5a4d1ea399-Paper.pdf>.
- Pavel Izmailov, Wesley J Maddox, Polina Kirichenko, Timur Garipov, Dmitry Vetrov, and Andrew Gordon Wilson. Subspace inference for bayesian deep learning. In *Uncertainty in Artificial Intelligence*, pages 1169–1179. PMLR, 2020.
- Xihaier Luo and Ahsan Kareem. Bayesian deep learning with hierarchical prior: Predictions from limited and noisy data. *Structural Safety*, 84:101918, 2020. ISSN 0167-4730. doi: <https://doi.org/10.1016/j.strusafe.2019.101918>. URL <https://www.sciencedirect.com/science/article/pii/S0167473019303820>.
- Christos Louizos, Karen Ullrich, and Max Welling. Bayesian compression for deep learning. *Advances in neural information processing systems*, 30, 2017.
- Vincent Fortuin. Priors in bayesian deep learning: A review. *International Statistical Review*, 2022.
- Eric Nalisnick, José Miguel Hernández-Lobato, and Padhraic Smyth. Dropout as a structured shrinkage prior. In *International Conference on Machine Learning*, pages 4712–4722. PMLR, 2019.
- Skyler Seto, Martin T. Wells, and Wenyu Zhang. *HALO: Learning to Prune Neural Networks with Shrinkage*, pages 558–566. doi: 10.1137/1.9781611976700.63. URL <https://epubs.siam.org/doi/abs/10.1137/1.9781611976700.63>.
- Soumya Ghosh, Jiayu Yao, and Finale Doshi-Velez. Structured variational learning of Bayesian neural networks with horseshoe priors. In Jennifer Dy and Andreas Krause, editors, *Proceedings of the 35th International Conference on Machine Learning*, volume 80 of *Proceedings of Machine Learning Research*, pages 1744–1753. PMLR, 10–15 Jul 2018. URL <https://proceedings.mlr.press/v80/ghosh18a.html>.
- Jasper Snoek, Oren Rippel, Kevin Swersky, Ryan Kiros, Nadathur Satish, Narayanan Sundaram, Mostofa Patwary, Mr Prabhat, and Ryan Adams. Scalable bayesian optimization using deep neural networks. In *International conference on machine learning*, pages 2171–2180. PMLR, 2015.
- Ranganath Krishnan, Mahesh Subedar, and Omesh Tickoo. Efficient priors for scalable variational inference in bayesian deep neural networks. In *Proceedings of the IEEE/CVF International Conference on Computer Vision (ICCV) Workshops*, Oct 2019.
- Erik Daxberger, Agustinus Kristiadi, Alexander Immer, Runa Eschenhagen, Matthias Bauer, and Philipp Hennig. Laplace redux - effortless bayesian deep learning. In M. Ranzato, A. Beygelzimer, Y. Dauphin, P.S. Liang, and J. Wortman Vaughan, editors, *Advances in Neural Information Processing Systems*, volume 34, pages 20089–20103. Curran Associates, Inc., 2021a. URL <https://proceedings.neurips.cc/paper/2021/file/a7c9585703d275249f30a088cebba0ad-Paper.pdf>.
- Ewan Cameron. A generalized savage-dickey ratio, 2013. URL <https://arxiv.org/abs/1311.1292>.
- MJ Rosa, K Friston, and W Penny. Post-hoc selection of dynamic causal models. *Journal of neuroscience methods*, 208(1):66–78, 2012.
- Karl Friston and Will Penny. Post hoc bayesian model selection. *Neuroimage*, 56(4):2089–2099, 2011.
- Karl J Friston, Vladimir Litvak, Ashwini Oswal, Adeel Razi, Klaas E Stephan, Bernadette CM Van Wijk, Gabriel Ziegler, and Peter Zeidman. Bayesian model reduction and empirical bayes for group (dcm) studies. *Neuroimage*, 128:413–431, 2016.
- Karl J Friston, Marco Lin, Christopher D Frith, Giovanni Pezzulo, J Allan Hobson, and Sasha Oudobaka. Active inference, curiosity and insight. *Neural computation*, 29(10):2633–2683, 2017.
- Karl Friston, Thomas Parr, and Peter Zeidman. Bayesian model reduction, 2018. URL <https://arxiv.org/abs/1805.07092>.

- Ryan Smith, Philipp Schwartenbeck, Thomas Parr, and Karl J Friston. An active inference approach to modeling structure learning: Concept learning as an example case. *Frontiers in computational neuroscience*, 14:41, 2020.
- Jim Beckers, Bart van Erp, Ziyue Zhao, Kirill Kondrashov, and Bert de Vries. Principled pruning of bayesian neural networks through variational free energy minimization. *arXiv preprint arXiv:2210.09134*, 2022.
- Manuel Haußmann, Fred A Hamprecht, and Melih Kandemir. Sampling-free variational inference of bayesian neural networks by variance backpropagation. In *Uncertainty in Artificial Intelligence*, pages 563–573. PMLR, 2020.
- Toby J Mitchell and John J Beauchamp. Bayesian variable selection in linear regression. *Journal of the american statistical association*, 83(404):1023–1032, 1988.
- Juho Piironen and Aki Vehtari. Sparsity information and regularization in the horseshoe and other shrinkage priors. *Electronic Journal of Statistics*, 11(2):5018–5051, 2017.
- Yann LeCun, Bernhard Boser, John S Denker, Donnie Henderson, Richard E Howard, Wayne Hubbard, and Lawrence D Jackel. Backpropagation applied to handwritten zip code recognition. *Neural computation*, 1(4):541–551, 1989.
- Alexey Dosovitskiy, Lucas Beyer, Alexander Kolesnikov, Dirk Weissenborn, Xiaohua Zhai, Thomas Unterthiner, Mostafa Dehghani, Matthias Minderer, Georg Heigold, Sylvain Gelly, et al. An image is worth 16x16 words: Transformers for image recognition at scale. *arXiv preprint arXiv:2010.11929*, 2020.
- Ilya O Tolstikhin, Neil Houlsby, Alexander Kolesnikov, Lucas Beyer, Xiaohua Zhai, Thomas Unterthiner, Jessica Yung, Andreas Steiner, Daniel Keysers, Jakob Uszkoreit, et al. Mlp-mixer: An all-mlp architecture for vision. *Advances in neural information processing systems*, 34:24261–24272, 2021.
- David M Blei, Alp Kucukelbir, and Jon D McAuliffe. Variational inference: A review for statisticians. *Journal of the American statistical Association*, 112(518):859–877, 2017.
- Matthew James Beal. *Variational algorithms for approximate Bayesian inference*. University of London, University College London (United Kingdom), 2003.
- Matthew D Hoffman, David M Blei, Chong Wang, and John Paisley. Stochastic variational inference. *Journal of Machine Learning Research*, 2013.
- Rajesh Ranganath, Sean Gerrish, and David Blei. Black box variational inference. In *Artificial intelligence and statistics*, pages 814–822. PMLR, 2014.
- John Schulman, Nicolas Heess, Theophane Weber, and Pieter Abbeel. Gradient estimation using stochastic computation graphs. *Advances in neural information processing systems*, 28, 2015.
- Eli Bingham, Jonathan P. Chen, Martin Jankowiak, Fritz Obermeyer, Neeraj Pradhan, Theofanis Karaletsos, Rohit Singh, Paul A. Szerlip, Paul Horsfall, and Noah D. Goodman. Pyro: Deep universal probabilistic programming. *J. Mach. Learn. Res.*, 20:28:1–28:6, 2019. URL <http://jmlr.org/papers/v20/18-403.html>.
- Juntang Zhuang, Tommy Tang, Yifan Ding, Sekhar C Tatikonda, Nicha Dvornek, Xenophon Papademetris, and James Duncan. Adabelief optimizer: Adapting stepsizes by the belief in observed gradients. *Advances in neural information processing systems*, 33:18795–18806, 2020.
- Igor Babuschkin, Kate Baumli, Alison Bell, Surya Bhupatiraju, Jake Bruce, Peter Buchlovsky, David Budden, Trevor Cai, Aidan Clark, Ivo Danihelka, Antoine Dedieu, Claudio Fantacci, Jonathan Godwin, Chris Jones, Ross Hemsley, Tom Hennigan, Matteo Hessel, Shaobo Hou, Steven Kapturovski, Thomas Keck, Iurii Kemaev, Michael King, Markus Kunesch, Lena Martens, Hamza Merzic, Vladimir Mikulik, Tamara Norman, George Papamakarios, John Quan, Roman Ring, Francisco Ruiz, Alvaro Sanchez, Rosalia Schneider, Eren Sezener, Stephen Spencer, Srivatsan Srinivasan, Wojciech

- Stokowiec, Luyu Wang, Guangyao Zhou, and Fabio Viola. The deepmind jax ecosystem, 2020. URL <http://github.com/deepmind>.
- Edward I George and Robert E McCulloch. Variable selection via gibbs sampling. *Journal of the American Statistical Association*, 88(423):881–889, 1993.
- Aryan Mobiny, Pengyu Yuan, Supratik K Moulik, Naveen Garg, Carol C Wu, and Hien Van Nguyen. Dropconnect is effective in modeling uncertainty of bayesian deep networks. *Scientific reports*, 11(1):5458, 2021.
- Jincheng Bai, Qifan Song, and Guang Cheng. Efficient variational inference for sparse deep learning with theoretical guarantee. *Advances in Neural Information Processing Systems*, 33:466–476, 2020.
- Aliaksandr Hubin and Geir Storvik. Variational inference for bayesian neural networks under model and parameter uncertainty. *arXiv preprint arXiv:2305.00934*, 2023.
- Sanket Jantre, Shrijita Bhattacharya, and Tapabrata Maiti. Layer adaptive node selection in bayesian neural networks: Statistical guarantees and implementation details. *arXiv preprint arXiv:2108.11000*, 2021.
- Yan Sun, Qifan Song, and Faming Liang. Learning sparse deep neural networks with a spike-and-slab prior. *Statistics & probability letters*, 180:109246, 2022.
- Xiongwen Ke and Yanan Fan. On the optimization and pruning for bayesian deep learning. *arXiv preprint arXiv:2210.12957*, 2022.
- Soumya Ghosh, Jiayu Yao, and Finale Doshi-Velez. Model selection in bayesian neural networks via horseshoe priors. *J. Mach. Learn. Res.*, 20(182):1–46, 2019.
- Matthew P. Wand, John T. Ormerod, Simone A. Padoan, and Rudolf Frühwirth. Mean Field Variational Bayes for Elaborate Distributions. *Bayesian Analysis*, 6(4):847 – 900, 2011. doi: 10.1214/11-BA631. URL <https://doi.org/10.1214/11-BA631>.
- Erik Daxberger, Agustinus Kristiadi, Alexander Immer, Runa Eschenhagen, Matthias Bauer, and Philipp Hennig. Laplace redux-effortless bayesian deep learning. *Advances in Neural Information Processing Systems*, 34:20089–20103, 2021b.
- Mohammad Khan, Didrik Nielsen, Voot Tangkaratt, Wu Lin, Yarin Gal, and Akash Srivastava. Fast and scalable bayesian deep learning by weight-perturbation in adam. In *International conference on machine learning*, pages 2611–2620. PMLR, 2018.
- Prajit Ramachandran, Barret Zoph, and Quoc V Le. Searching for activation functions. *arXiv preprint arXiv:1710.05941*, 2017.
- Dan Hendrycks and Kevin Gimpel. Gaussian error linear units (gelus). *arXiv preprint arXiv:1606.08415*, 2016.